Sedimentary Geology 220 (2009) 12–28

Contents lists available at ScienceDirect

Sedimentary Geology

journal homepage: www.elsevier.com/locate/sedgeo

Cliff-top storm deposits on Banneg Island, Brittany, France: Effects of giant waves in the Eastern Atlantic Ocean

Serge Suanez [a,*], Bernard Fichaut [a,1], Rudy Magne [b,2]

[a] GEOMER – UMR 6554 CNRS LETG, Institut Universitaire Européen de la Mer, Place Nicolas Copernic, 29280 Plouzané, France
[b] SHOM (SHOM/HOM/REC – Vagues et domaine littoral), 13 rue du Chatellier, 29609 Brest Cedex, France

ARTICLE INFO

Article history:
Received 27 June 2008
Received in revised form 24 February 2009
Accepted 10 June 2009

Keywords:
Cliff-top storm deposits
Imbricate boulders
Giant waves
Storms
Brittany
France

ABSTRACT

This study is based on the morphosedimentary analysis of the cliff-top storm deposits accumulated on the coast of Banneg Island located in the archipelago of Molène (Brittany, France). These CTSDs comprise large, tabular clasts quarried from the upper part of the cliff and the backing scoured platform by giant oceanic storm waves impacting directly the western coast of the island. An analysis of the distribution and the geomorphology of these accumulations were carried out using the DGPS topographic surveys. Most of the clasts are organised into imbricate boulder clusters or ridges deposited between 7.5 and 14.5 masl. 52 accumulations were inventoried from the north to the south of the island, representing a global volume of 1000 m^3. The median size of the clasts calculated is equivalent to 0.8 × 0.6 × 0.4 m and a weight of 0.6 t. The largest one measuring 5.3 × 3.9 × 0.5 m (≈32 t) is located in the centre of the island (ridge #28). It has been deposited 14 m inland from the edge of the cliff at the elevation of 9 m. Sediment analysis shows that clast sizes become smaller with increasing distance from the shoreline, but there is no relationship between the sorting and the distance inland. A study of the hydrodynamic conditions inducing clast transport was undertaken by an analysis of the wave data from the 1989 to the 1990 winter storms. Models of wave runup indicate that their highest water levels may have reached up to 19 masl, 5 to 10 m higher than the top of the cliff. Submersion by giant storm waves has been more important and frequent in the centre and the south of the island. Wave data over the 1979 to the 2007 period shows that no events as powerful as those of the 1989 to the 1990 winter were recorded during the last 30 years. Yet, it appears that the 1979–1990 decade was characterized by important morphogeneous events while the following period (1990–2007) has experienced a sharp decrease in storm events. These variations could be attributed to the inversion from a negative towards a positive phase in the North Atlantic Oscillation index.

1. Introduction

Large clast accumulations on the tops of the high rocky cliffs have been recognized on the Atlantic and northern North Sea coasts of the British Isles (Williams and Hall, 2004). These deposits have been described as a result of the giant storm waves and they have been referred to as the cliff-top storm deposits (CTSDs) (Hall et al., 2006; Hansom and Hall, 2009; Hall et al., 2008; Hansom et al., 2008). As described by Hall et al. (2006), the CTSDs generally occur on cliffs at an elevation of 20 m above sea level and may occasionally reach up to 50 m at exposed sites on the deep-water coasts. They are generated largely by the quarrying of blocks from the upper part of the cliff, and transported by wave runup across cliff-top platforms and ramps to be deposited inland. Therefore, the CTSDs comprise angular blocks characterized by the lack of sorting and large size. The largest clast measured on the Aran Island was approximatively 96 m^3 (Williams and Hall, 2004), they may reach 277 m^3 (Hansom et al., 2008). CTSDs are accumulated back from the cliff edge behind cliff-top rock surfaces swept clear of debris by a storm activity (wave-scoured supratidal platform or ramp). They form different features such as steep-faced ridges composed of seaward-dipping imbricate clasts, but also clusters, spreads and individual clasts. As it was noticed by Williams and Hall (2004), this organisation into ridges, may require repeated reworking by waves rather than the rare impact of a train of tsunami waves. Imbricate fabric has been also interpreted as repeated accumulation processes due to storm waves inducing staking of the clasts against each other so that one of the clast axes dips with respect to the horizontal. Field observations and modelling allowed us to link wave processes to quarrying, transportation and deposition of boulders on top of cliffs (after Noormets et al., 2004; Hansom et al., 2008). Incident waves at the same height as the cliff edge or lower, produce pressures sufficient to promote detachment and lifting of large blocks. Where wave crest elevation exceeds cliff-top height, high flow velocities accelerate and allow transportation and deposition of blocks inland at the limit of runup.

* Corresponding author. Tel.: +33 2 98 49 86 10; fax: +33 2 98 49 87 03.
E-mail addresses: serge.suanez@univ-brest.fr (S. Suanez), bernard.fichaut@univ-brest.fr (B. Fichaut), rudy.magne@shom.fr (R. Magne).
[1] Tel.: +33 2 98 49 86 10; fax: +33 2 98 49 87 03.
[2] Tel.: +33 2 98 22 06 84; fax: +33 2 98 22 18 64.

0037-0738/$ – see front matter © 2009 Elsevier B.V. All rights reserved.
doi:10.1016/j.sedgeo.2009.06.004

Until now the CTSDs in the Eastern Atlantic Ocean have been recognized only in the northern British Isles, in northern Scotland (Orkney and Shetland Islands) and off the western seaboard of Ireland (Aran Islands). However, clast accumulations occur on the tops of cliffs on Banneg Island in the archipelago of Molène, off the western seaboard of Brittany (Fig. 1). These accumulations were reported for the first time by Hallégouët (1982a, 1984) in a frame of a broad geomorphological analysis of the archipelago of Molène. Later, in 1990, a new study of these deposits was undertaken after the large storm events that occurred during the winter of 1989–1990 (Fichaut and Hallégouët, 1989). Following these earlier studies, the distribution, geomorphological setting, sedimentology and hydrodynamic conditions were analysed in detail by using new methods of monitoring. The aim of this study is to determine whether these clast accumulations are CTSDs (as per the definition of Hall et al., 2006), and to provide new information about morphological effects of the ocean-sourced high-energy storm events on the Eastern Atlantic coasts. It is based on:

1. the morphosedimentary analysis of these deposits by using new investigation methods based on the DGPS measurements. These topographic surveys allowed to map and quantify volumes of these accumulations.
2. the study of the shape and the size characteristics of clasts based on the measurements of 908 blocks. This large sample of clasts enabled us, for the first time, to complete a detailed and quantitative analysis of the clast size.
3. the analysis of the hydrodynamic processes inducing clast dislodgement and displacement. The emphasis was put on analysis of the extreme water level associated with wave runup since it was described as a main parameter explaining the movement and the emplacement of large clasts and/or boulders (Dawson, 1994; Nott, 1997; Noormets et al., 2004).
4. an inventory of potential ocean-sourced high-energy events by analysing wave and tide conditions in the Iroise Sea over the last 30 years (1979–2007).

2. Geologic, geomorphologic and hydrodynamic setting

Banneg Island is located at the north-western limit of the archipelago of Molène in Iroise Sea at the tip of western Brittany (Fig. 1). This archipelago consists of 19 small islands totalizing a surface of 195 ha. They represent the summits of a large shallow submerged plateau covering 15,000 ha from low tide level to the depth of 10 m (Guilcher, 1959; Hallégouët, 1982b). Banneg Island has a particularly exposed situation on the edge of the deep Fromveur channel which separates the archipelago from Ouessant Island. On Banneg, from east to west coastal features and deposits show significant differences which are controlled by the exposure of the coast relative to dominant waves. The eastern sheltered coast presents a morphology characterized by gentle slopes and no cliffs. It is mainly constituted by shingle beaches and small sheet-sand accumulations. On the contrary, the exposed western coast is formed by steep cliffs up to 10 to 14 m NGF high that rise up to 6.5 to 10.5 m above high spring

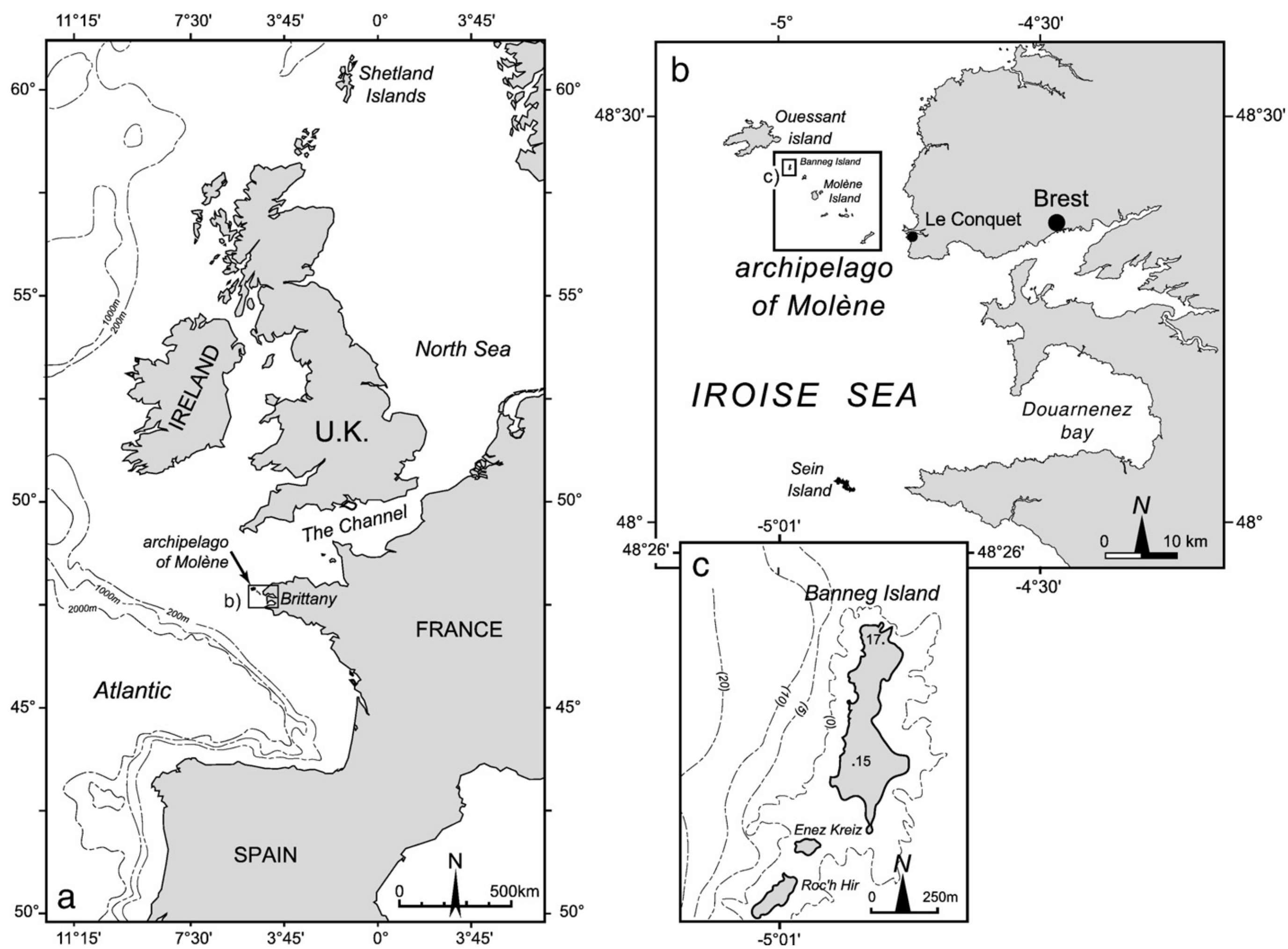

Fig. 1. The general location (a), the archipelago of Molène (b), and the study area of Banneg Island (c).

tide water level (altimetric reference NGF —*Nivellement Général Français*— refers to the topographic French datum. In our case this reference, altitude 0, is situated at 3.5 m above the low spring tide water level. In the present article, all elevations indicated above sea level (asl) will refer to this 0 NGF).

The rock cliffs of Banneg Island are cut in the Ploudalmézeau Leucogranite of the Palaeozoic age. It presents an orthogonal tabular structure due to the horizontal bedding and subvertical cracks and joints affecting the granite bedrock. The partial detachment of clasts by weathering processes along these joints and cracks facilitates their complete detachment from the cliff edge by the breaking waves.

The Iroise Sea is characterized by the semidiurnal tide regime. Tide range extends from 3 m in neap tide condition (coefficient 45) to 7 m in spring tide condition (coefficient 120). Therefore, the extreme high tide level is situated at about 3.50 m above the French datum topographic reference. The archipelago is directly influenced by westerly and north-westerly Atlantic waves (270° to 310°) which represent 60% of the annual regime and are very energetic (Fig. 2). South-western waves are also well represented, accounting for 20% of the annual regime. The most frequent significant wave height is approximately 1.5 m and represents 30% of the annual regime. The most frequent maximum wave heights (which represent 25 to 30% of the annual regime) reach 2.5 m, although they may exceed 16 to 18 m. The most frequent significant wave periods are between 8 to 9 s and they represent 30% of the annual regime. The most frequent maximum wave periods reach 13.5 s, and range to 24 s. Because of the localisation of the island on the edge of the Molène continental shelf, offshore slopes are steep (Fig. 2). Immediately fronting the base of the cliff, 10% slopes occur from 0 to 250 m offshore, and then decrease gradually to 5% at 2000 m offshore where water depth reaches 50 m. Therefore, wave attenuation is very low inducing a high-energy of wave breaks.

3. Field observation: evidence of megaclast movement

The erosion of the western coast involves the detachment of the tabular clasts and transport inland (Fig. 3a). The clasts form imbricate clusters and/or trains. They have been described for the first time at the beginning of the 1980s (Hallégouët, 1982a, 1984). As mentioned in the Introduction, the first observations of clasts movement were carried out in spring 1990 in order to evaluate the morphological effect of the major storms on Banneg Island, during the winter of 1989–1990 (Fichaut and Hallégouët, 1989). The authors showed that the most important changes occurred in the central part of the island which was submerged by seawater. In this area, several tonnes of blocks were detached from the

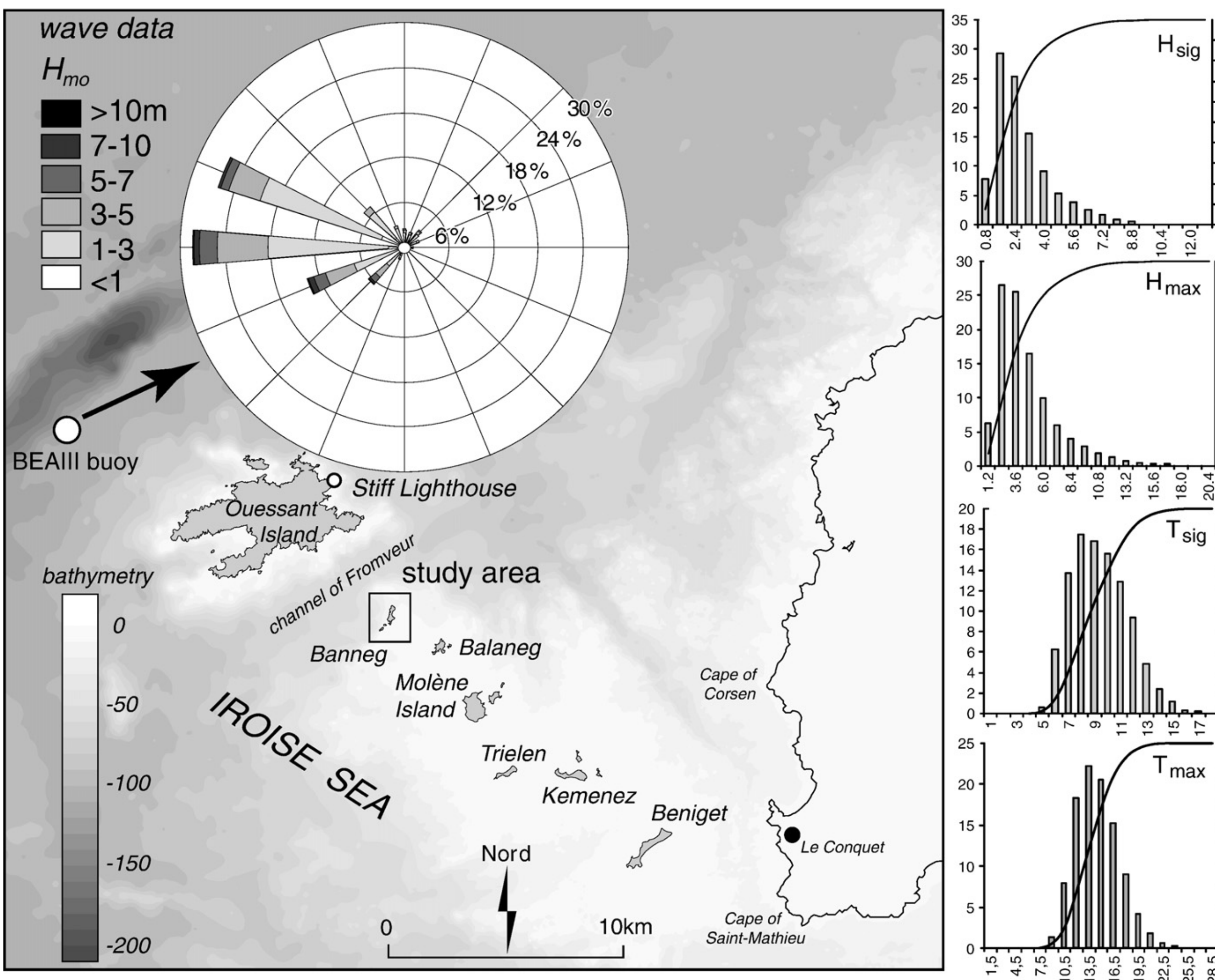

Fig. 2. Wave climate of the Iroise Sea. Histograms of significant wave heights H_{sig} and maximum wave heights H_{max} and significant wave periods T_{sig} and maximum wave periods T_{max} established from data obtained by buoy measurements (buoy BEAIII) off Ouessant Island between 30/08/1985 and 17/08/2001 (source: site Candhis du CETMEF — http://www.cetmef.equipement.gouv.fr/donnees/candhis/home.php); deep-sea wave directions off Ouessant Island (at the location of the buoy BEAIII) obtained by numerical run model over the period 1979–2002 (source: *Laboratoire National d'Hydraulique et d'Environnement*, LNHE-EDF Chatou, and *Centre d'Etudes Techniques Maritimes Et Fluviales*, CETMEF-Brest).

Fig. 3. a) Cliff-top clast deposits on the western coast of Banneg Island. b) Southward view of the north–centre sector in April 1990. Regolith stripped of vegetation and lichen free freshly deposited clasts in clusters #15 and 16 show that powerful flows crossed the island from west to east. 1: southern limit of regolith stripped of vegetation. 2: lichen free clasts. c) In the centre sector, a channel has been incised into bedrock by water exiting eastward. Cluster #18 appears in the middle of the view. d) April 1990, eastern shoreline of Banneg island downstream of central and northern central areas. The shingle beach ridge has been pushed offshore by the flow that also carried angular blocks from the western cliff. e) Clast displaced during a storm in the autumn of 2005.

seaward edge of the cliffs and the cliff-top scoured platforms prior to transportation in the inner part of the island (Fig. 3b). The clast movements were initiated by flows generated by cliff-top bores following the wave breaks on the top of the cliffs. In the central part of the inland, the torrential flows of exiting water induced strong soil erosion (Fig. 3b), and a pre-existent spillway was deepened by an incision into the bedrock (Fig. 3c). Through this gully (1 to 1.5 m deep and 10 to 15 m wide), some of the blocks detached from the edge of the western cliff were transported to the eastern coast of the island where they were incorporated into the existing shingle beach ridge (Fig. 3d). This shingle ridge was pushed seaward, 10 m away from its previous location (Fig. 3d).

More recently, field surveys showed that several blocks were dislodged and moved from the edge of the western cliff between October and December 2005. One of them, 1.7 m long, 1 m wide, and 0.5 high, weighing approximately 2.6 t, was quarried at 10 masl and then deposited 12 m further inland from the edge of the cliff after a rebound leaving a chatter mark at 12 masl (Fig. 3e).

4. Purpose and methods

4.1. Morphosedimentary analysis

The morphological study of clast accumulations was based on the DGPS topographic measurements carried out between October 2005 and June 2006. More than 15,000 measurements were realised to analyse topographic distribution, orientation and morphological

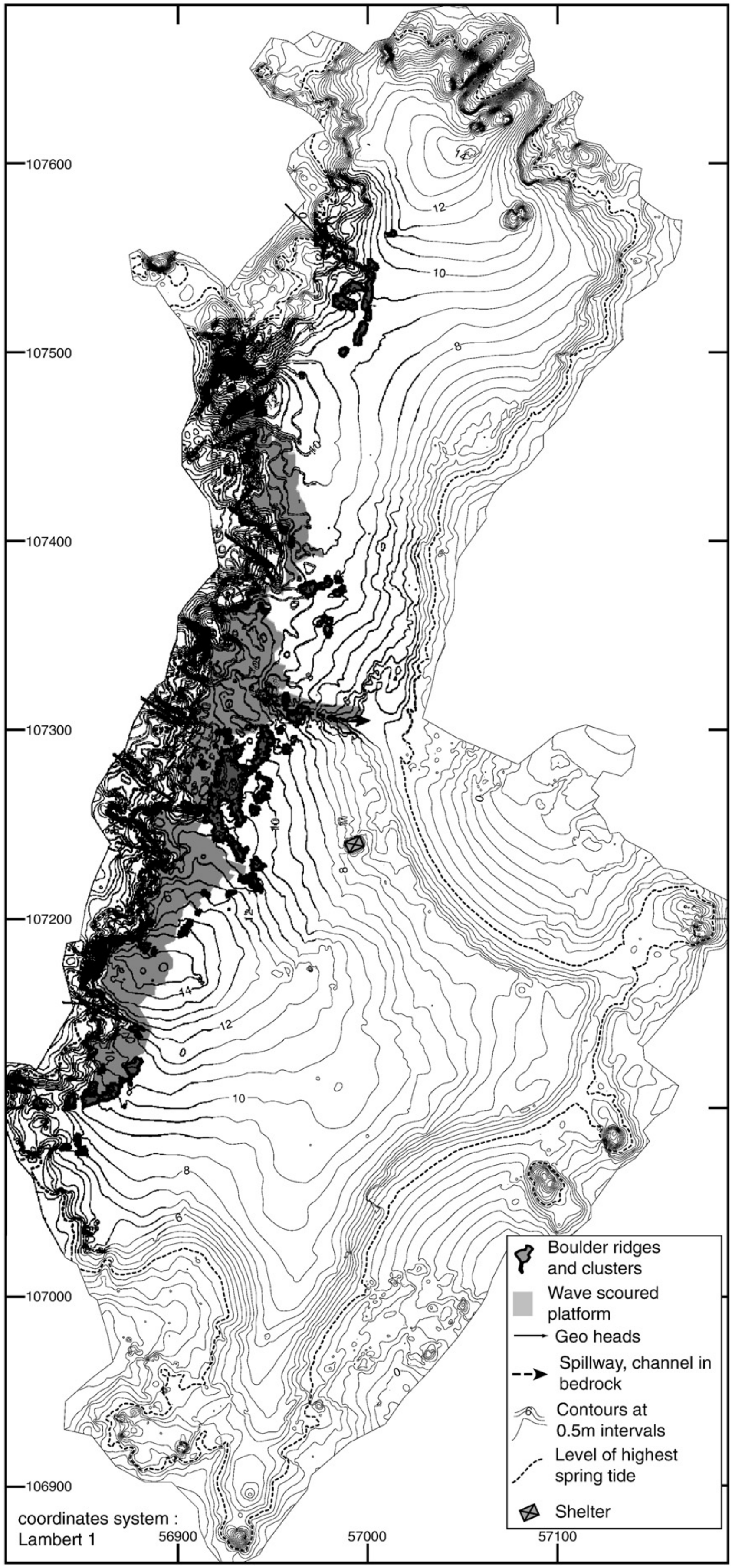

Fig. 4. Topography of Banneg and localisation of main geomorphic features.

features of the clast deposits. A topographic survey of the entire island was also undertaken to determine altitudes where clasts are accumulated, and analyse the morphology of the cliff exposed to the erosion and the displacement processes. Trimble 5700/5800 Differential GPS was used to collect data points in Real Time Kinematics (RTK) mode with an accuracy of 0.015 m in (x, y) and 0.02 m in (z). Each DGPS measurement was calibrated using geodesic marker from the French datum and geodesic network provided by the IGN (*Institut Géographique National*). A Digital Elevation Model was computed on Surfer 8.0 software by applying an algorithm based on a kriging method supporting breaklines. A grid of 0.5×0.5 m spacing was used to produce accurate topographic data. A Digital Elevation Model was used to establish a map with contour lines from which, morphologic analysis was done (Fig. 4). Banneg totalizes 52 clusters and ridges, representing 1000 m^3.

The sedimentary analysis was carried out by measuring the size of the 908 clasts, using the triaxial measurements (i.e. a-axis (long), b-axis (intermediate), c-axis (short)), in 16 of the 52 accumulations of the north, centre, centre–south1 and south sectors. These accumulations are the largest ones and represent 2/3 of the total volume of clasts (731 m^3, see Fig. 7). This sample set can be considered as the representative as long as the accumulations of the centre–north and centre–south2 represent only 8% of the total volume of deposits. This sedimentary analysis allowed us to determine the shape of the blocks (angularity, roundness, tabular), and clast size distributions and sorting (Table 1). Sorting has been obtained by calculating the coefficient of variation which describes the magnitude sample values and the variation within them. This is the ratio of standard deviation to the mean:

$$V_c = \frac{\sigma}{\overline{X}} \tag{1}$$

where V_c is the coefficient of variation; σ is the standard deviation; and $\overline{X}$ is the mean.

In order to analyse the imbricate fabric, seaward dips were also established by measuring the orientation of the a-axis and/or b-axis plane, which generally reflect the direction of the regional wave patterns that created the ridges.

4.2. Runup calculation defining extreme water level

The analysis of the hydrodynamic conditions was based on the estimation of an extreme water level as the factor controlling the clast detachment and the transport. It was undertaken by analysing the 1989–1990 winter storms as far as it was shown that important clast movements took place during these events (Fichaut and Hallégouët, 1989). Three major storms occurred during this period (Fig. 5). The first one, lasting from the 13 to 17 of December 1989 was characterized by significant wave heights reaching 18 m and surge close to 0.90 m. During this event, the atmospheric pressures decreased below 970hpa and wind speed reached 25 m/s. The second event took place from the 23 of January to the 14 of February 1990. It was characterized by significant wave heights reaching 16 m and 18 m, and by speed wind exceeding 25 m/s several times. Barometric pressures equal to 985 hpa generated "barometric setup" reaching 0.50 m. The last storm event occurred at the end of February 1990 and was characterized by smaller significant wave heights reaching 12 m. On the contrary, the highest tide levels reaching 4 m IGN were recorded during this last event.

Through the study of these data, the aim of this analysis was to determine if the extreme water level was sufficiently high to exceed the height of cliffs. Two parameters were taken into account: the surge given by tide records and the wave runup. The latter component was calculated using the Mase (1989) formula generally employed for irregular waves breaking on slopes of $0.03\le\tan\beta\le0.2$ and the wave steepness, H_o/L_o of $0.07\le H_o/L_o\le0.07$:

$$\frac{R^T_{\max}}{H_{\mathrm{sig}}} = 2.32\ \xi_o^{0.77} \tag{2}$$

$$\frac{R^T_{2\%}}{H_{\mathrm{sig}}} = 1.86\ \xi_o^{0.71} \tag{3}$$

where $R^{\mathrm{T}}_{\max}$ corresponds to the highest runup; $R^{\mathrm{T}}_{2\%}$ corresponds to the 2% excess runup height; H_{sig}: deep water significant wave height; constant parameter $C=2.32$ for $R^{\mathrm{T}}_{\max}$ and 1.86 for $R^{\mathrm{T}}_{2\%}$; ξ_o: d'Iribarren number (Battjes, 1974):

$$\xi_o = \frac{\tan\beta}{(H_{\mathrm{sig}}/L_o)^{1/2}} \tag{4}$$

Results are listed in Table 1. Because of slope variation from the north ($\tan\beta$ 0.02) to south ($\tan\beta$ 0.05), runup $R^{\mathrm{T}}_{2\%}$ reaches respectively 7 m and 13.5 m NGF. The values obtained concerning runup $R^{\mathrm{T}}_{\max}$ are respectively equal to 7.7 m and 15.7 m NGF.

Table 1
$R^{\mathrm{T}}_{2\%}$ and $R^{\mathrm{T}}_{\max}$ runup values calculated according to two different slope components: $\tan\beta$ 0.02 to the north ; $\tan\beta$ 0.05 to the south.

S ($\tan\beta$)	H_{mo} (m)	T_{pic} (s)	ξ_o	$R^{\mathrm{T}}_{2\%}$	$R^{\mathrm{T}}_{\max}$
0.02 (North)	Max. 17.7	Max. 20	Max. 0.29	7 m	7.7 m
0.05 (South)			Max. 0.73	13.5 m	15.7 m

5. Results

5.1. Morphological setting of megaclasts

Clast deposits usually occur back from the cliff edge, behind rock surfaces that are largely swept clear of debris by the storm wave activity. This zone corresponds to the wave-scoured platform described by Hall et al. (2006). They form several ridges or clusters resting between 7.5 and 14.5 m NGF, e.g. 4 m to 11 m above the high spring tide water level (Fig. 6). In detail, 52 boulder accumulations were inventoried from the north to the south of the island, representing a global volume of 1000 m^3 (Fig. 7c). Nevertheless, this volume is an underestimate since all the isolated blocks scattered inland, far from the cliff edge, have not been measured.

These 52 boulder accumulations have been divided into 6 groups mainly located at the rear of coves separated by the headlands (Fig. 7a). They are erected into ridges forming either an arc like in the south (Fig. 8a), or elongated trains parallel to the coast like in the centre and the central-south1 (Fig. 8b). Locally, they also correspond to the isolated or the individual clusters. The boulder accumulations #4, #11, #29 and #45 are situated immediately on the edge of the cliff (Fig. 6a,d,h, and o) at the mouth of the geo heads (Figs. 4 and 7) which correspond to the major cracks oriented NW, and enlarged by marine erosion. These geos are characterized by the gentle slope <33% and may be compared to the "launching pads" concentrating wave breaks and therefore enhancing the potential for block movement (Fig. 4). The largest accumulations, representing 2/3 of the total, are located in the centre and the central-south1 areas (Fig. 7c). For instance the ridge #28 is 60 m long and 20 m wide (Figs. 6g and 8c). It is also in these areas that their arrangement is the most remarkable owing to the fact that they locally form triple parallel ridges (Fig. 6e) distinctly separated by the bare areas of bedrock or turf (Fig. 8d).

Neither the volume of the clast accumulations, nor the distance of their deposition inland from the cliff edge is correlated to the height and slope of the cliff (Fig. 9a and b). There is not either any correlation between the distance inland at which clasts are deposited and the height and the

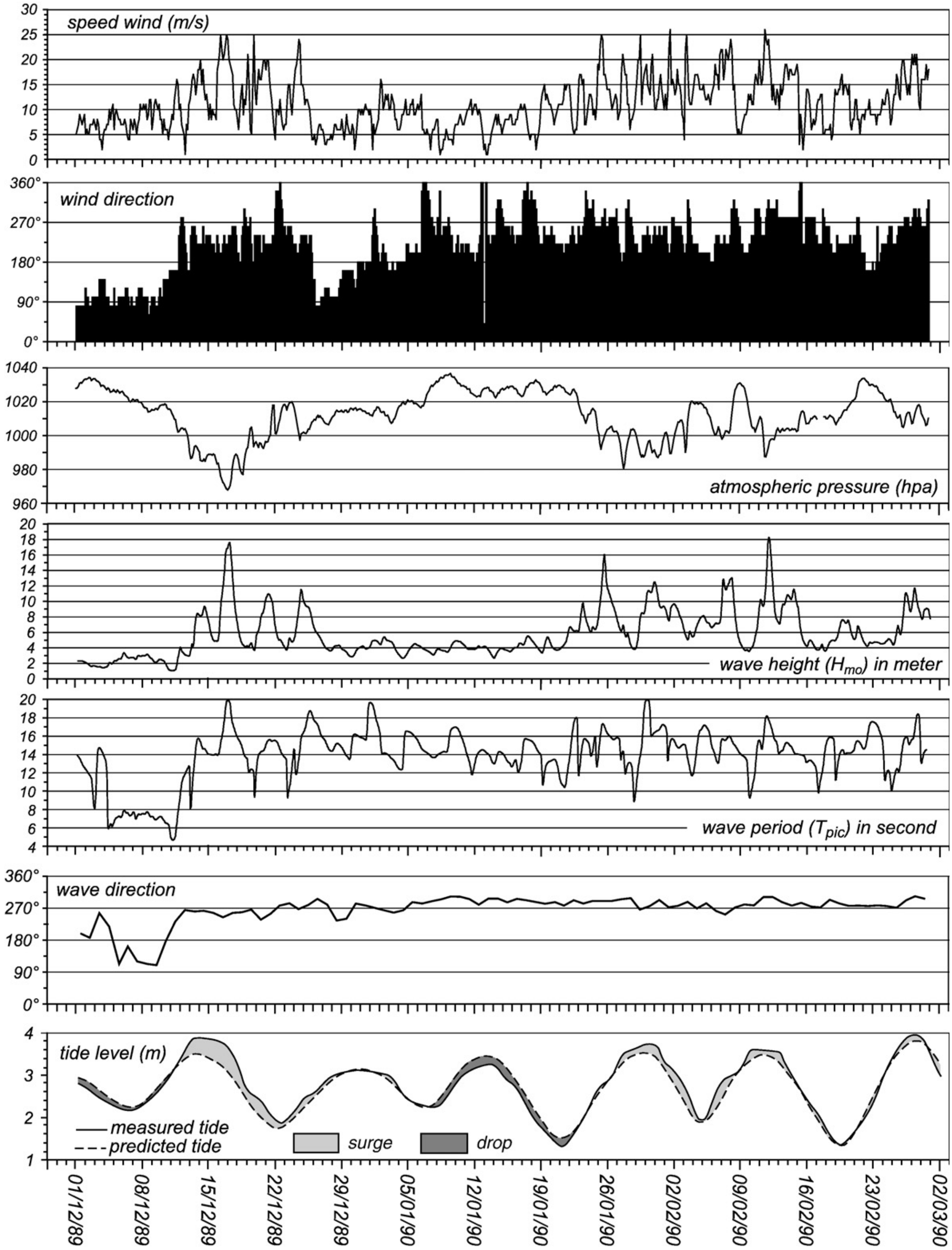

Fig. 5. Meteorological and oceanic characteristics (wave, wind, pressure and surge) recorded during the 1989–1990 winter storms. Wave data obtained from measurements by buoy BEAIII off Ouessant Island (lat. 48°30′; long. 5°45′; 110 m depth), wind and pressure data obtained from meteorological station *Météo France* of Ouessant Island (Stiff lighthouse), tide data obtained from the tide gauge station of Le Conquet (SHOM — lat. 48°21′; long. 4°46′).

slope of the cliff (Fig. 9c and d). In fact, the western coast is divided into cells individualised by their own hydrodynamic characteristics, mainly related to the morphology of the shoreface zone at the base of the cliff.

5.2. Clast imbrication

From the central to the south sectors, the clasts deposited exhibit an imbricate fabric (Fig. 8b,c and e). As reported by Williams and Hall (2004) on the Aran Islands, this fabric is best developed on the seaward margins of the ridges or clusters and is replaced by a more chaotic clast arrangement in a landward direction. As it was mentioned earlier, imbricate patterns were analysed establishing seaward dips by measuring the orientation of the *a*-axis and/or *b*-axis plane of the clasts. Fig. 7b shows clearly that the dominant imbrication direction of the deposits varies from 270° to 330°. This suggests, that the clast accumulations hold a record of storm waves from a range of directions. However, these directions have been locally modified on a local scale by reworking around embayments so that the imbrication forms an arc which reflects the shape of the bay. This is clearly the case in the central–south and south sectors (Fig. 7b). On the contrary, in the centre sector where the coastline is linear, directions are clearly 270°, coinciding with the dominant wind-driven wave direction (Fig. 2).

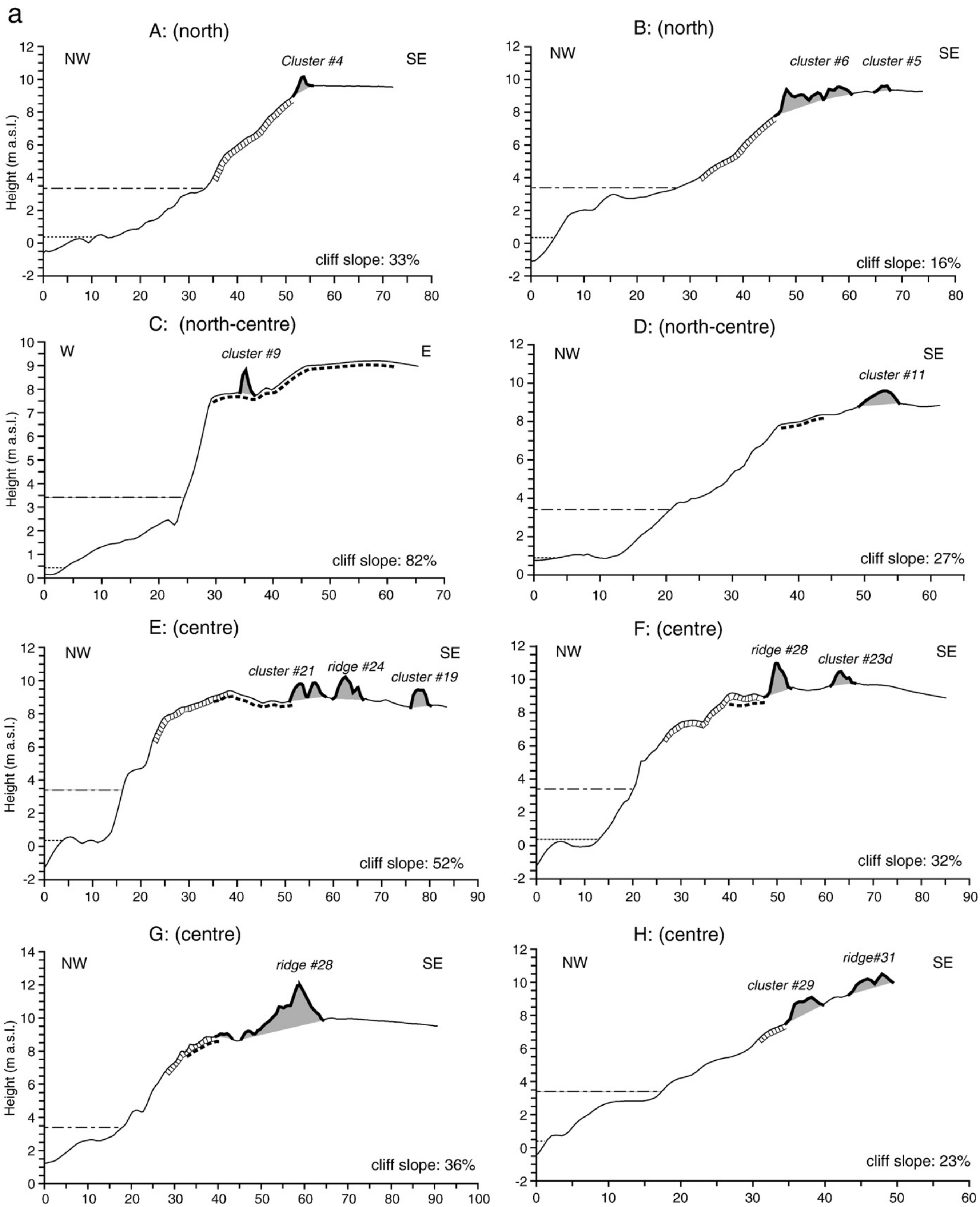

Fig. 6. Cliff transects on the western coast of Banneg.

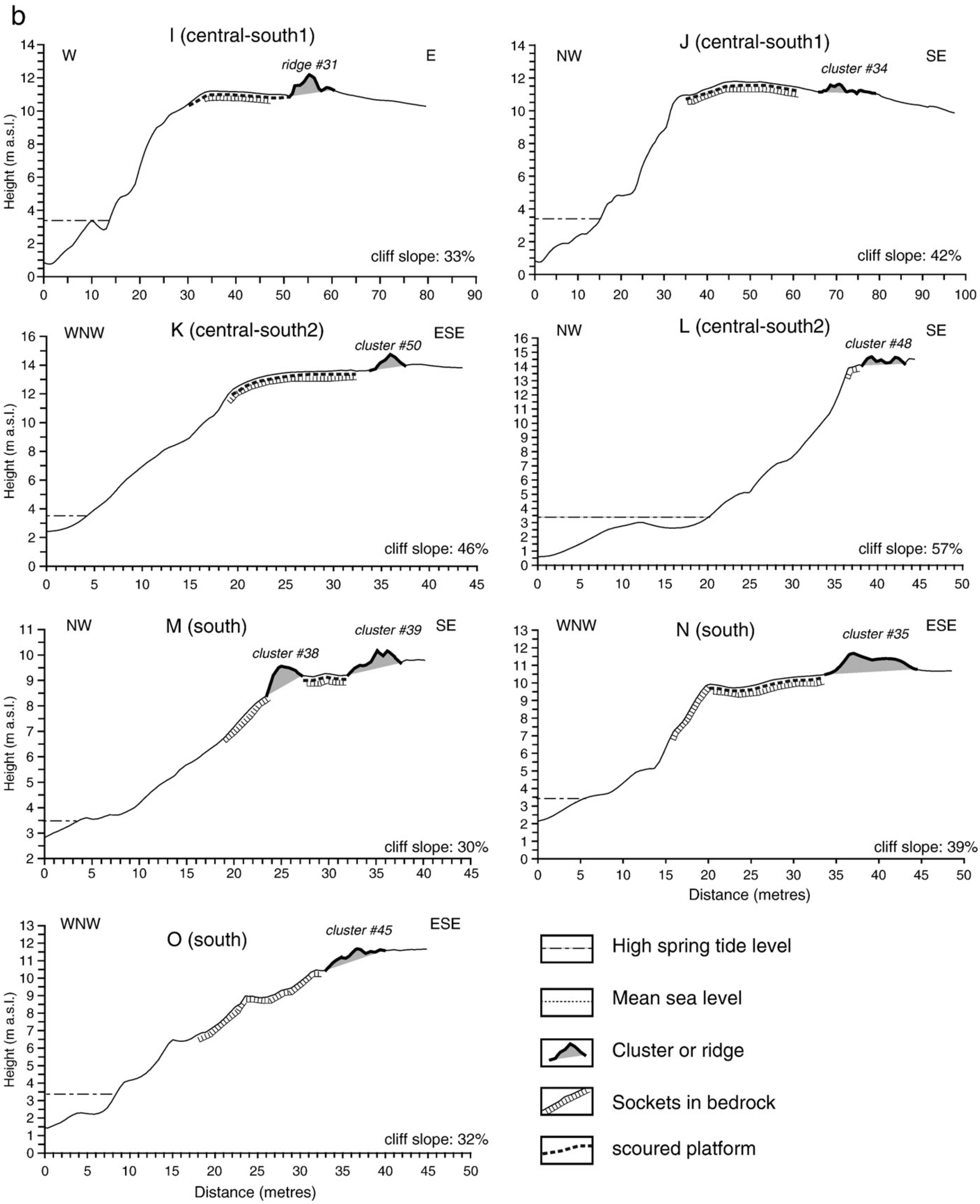

Fig. 6 (*continued*).

5.3. Shape and size analysis of clast deposits

Most clasts have a distinctly rectangular, wedge shape with a flat base and flat sides. As exposed previously, they correspond to tabular blocks which are mostly quarried from the upper part of the rocky cliff (Fig. 9a) and the scoured platform (Fig. 9b). Sockets that have been monitored show that quarrying ranges in between 4 and 14 masl (Fig. 6). As it appears on Fig. 9a, the horizontal and the subhorizontal joints are

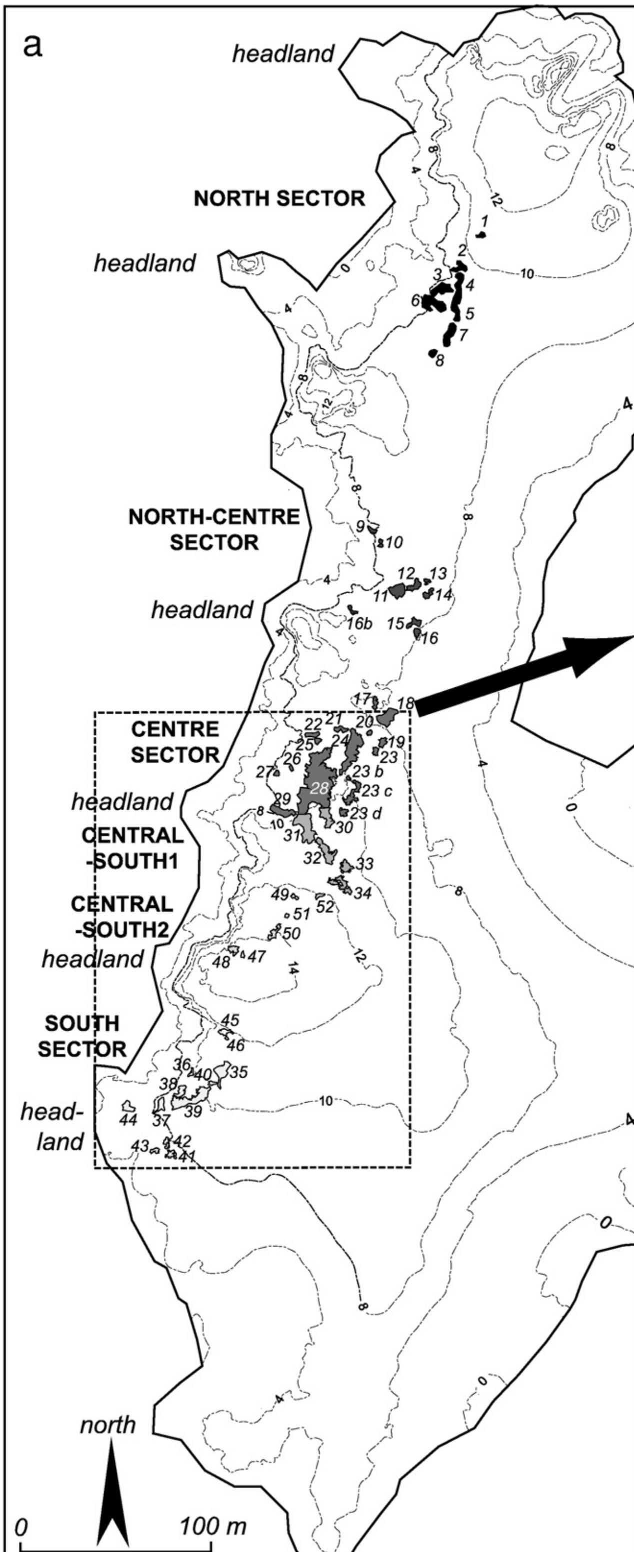

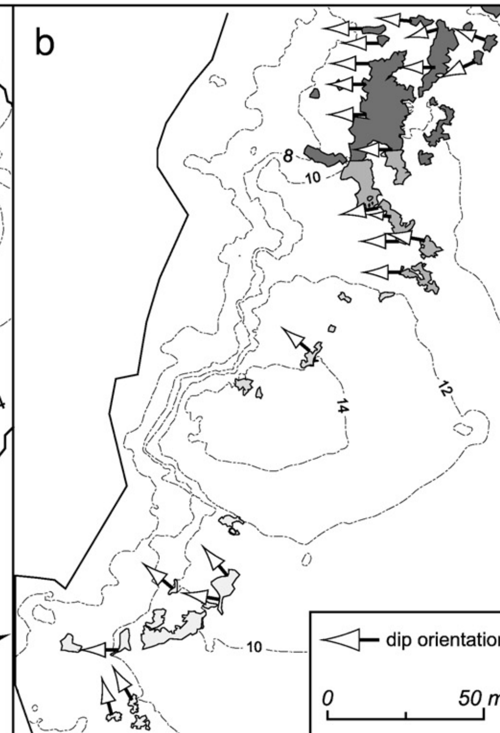

Sector	Number	Volume (m^3)
NORTH	1	2
	2	9
	3	22
	4	16
	5	2
	6	38
	7	12
	8	3
TOTAL NORTH :		**104**
NORTH-CENTRE	9	7
	10	4
	11	23
	12	11
	13	2
	14	7
	15	7
	16	3
	16 b	4
TOTAL NORTH-CENTRE :		68
CENTRE	17	7
	18	12
	19	8
	20	3
	21	8
	22	8
	23	4
	23 b	1
	23 c	13
	23 d	4
	24	91
	25	5
	26	2
	27	4
	28	357
	29	29
TOTAL CENTRE :		556

Sector	Number	Volume (m^3)
C. SOUTH1	30	41
	31	48
	32	22
	33	6
	34	11
TOTAL CENT. SOUTH1 :		128
C. SOUTH2	47	1
	48	6
	49	2
	50	6
	51	1
	52	2
TOTAL CENTRE-SOUTH2 :		18
SOUTH	35	35
	36	4
	37	23
	38	8
	39	25
	40	2
	41	5
	42	4
	43	3
	44	15
	45	5
	46	3
TOTAL SOUTH :		132

TOTAL VOLUME 1006 m^3

c

Fig. 7. Characteristics of clast deposits on Banneg Island. a) Location. b) Wave direction based on dip measurements. c) Volume of clast accumulations.

much larger than the vertical ones. Therefore, quarrying tends to produce tabular blocks that differ radically from the ones that lay at the base of the cliffs, which are overwhelmingly rounded in shape (Fig. 9c). These processes have been particularly well described by the clast deposit studies in the North Atlantic coast (Dawson and Shi, 2000; Williams and Hall, 2004; Hall et al., 2006) and in the Pacific (Jones and Hunter, 1992; Noormets et al., 2002, 2004; Whelan and Keating, 2004).

The sedimentary analysis shows a median size equal to $0.8 \times 0.6 \times 0.4$ m and a weight of 0.6 t (Table 2). Yet, the clasts vary considerably in size from one sector to the other with the largest one measuring $5.3 \times 3.9 \times 0.5$ m and weighing approximately 32 t (Fig. 9d). It is a large tabular clast and it is located in the centre of the island (imbricated clast #28). It has been deposited 14 m inland from the edge of the cliff at the altitude of 9 m. 65 of the 91 blocks (72%) of

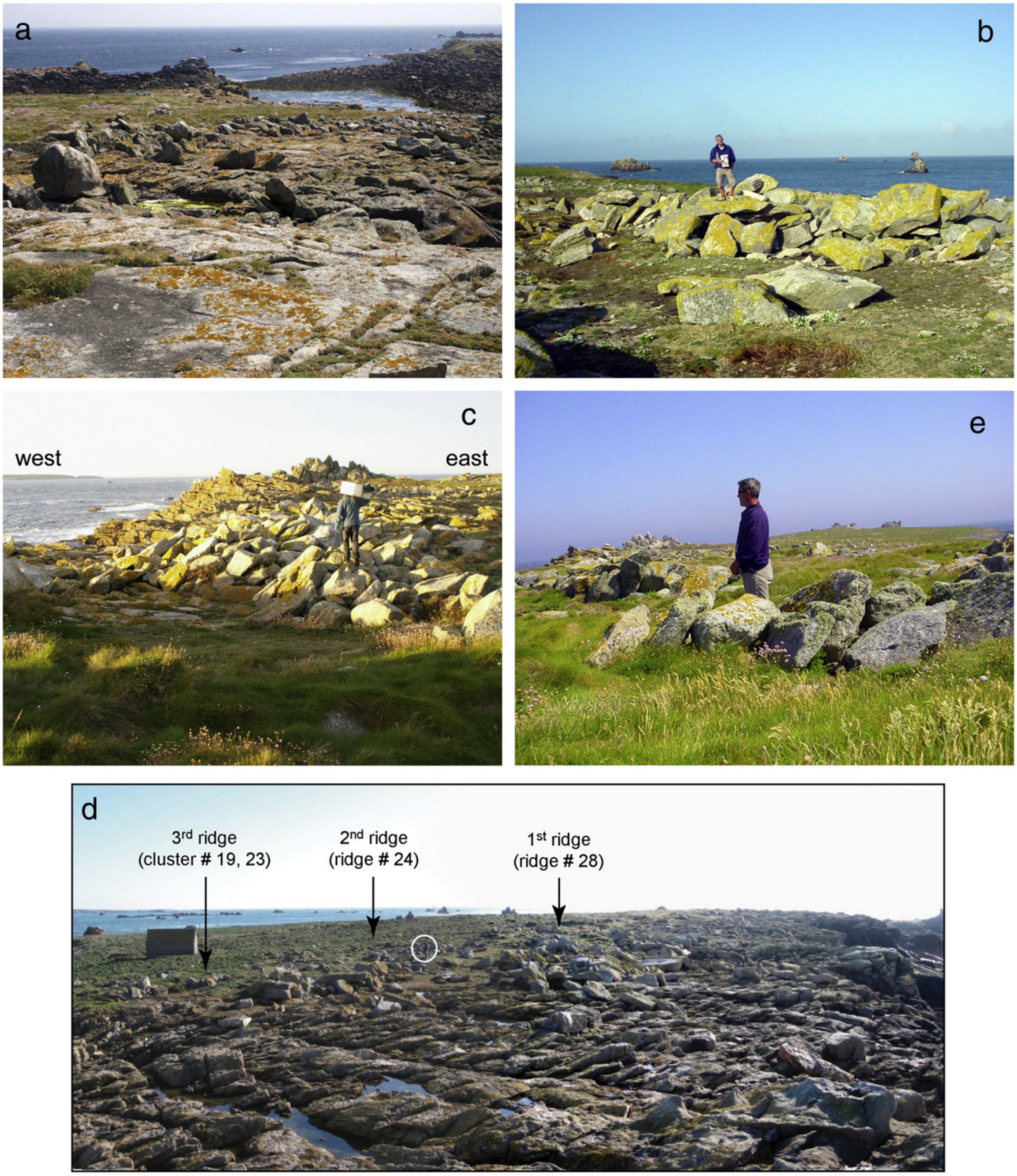

Fig. 8. Morphological arrangement of clast deposits. a) Train of imbricated clasts forming an arc in the south area. b) Imbricated clasts forming elongated train parallel to the coast in the central area. c) Clast accumulation #28 located in the centre of the island. The largest of Banneg. d) Clast accumulations forming triple ridges parallel to the cliff edge in the central area. e) Largest clast located on the centre of the island (imbricated clast #28) measuring 5.3 × 3.9 × 0.5 m and weighing approximately 32 t. e) Seaward dip of imbricated clasts indicating wave direction linked to sedimentation processes.

which the weight exceeds the last decile (90th percentile) e.g. >3 t, are located in the centre sector whereas this sector totalizes only 38% of the total sample.

The analysis shows that the clast size decreases with the increasing distance from the shoreline. This result confirms observations made by many authors on some other studied areas (Bryant et al., 1992; Dawson, 1994; Nanayama et al., 2000). On the contrary, there is no relation between the sorting and the distance inland. These last results contradict observations made by several authors attesting that the clasts are generally better sorted when the distance inland increases (Bourrouilh-Le Jan and Talandier, 1985; Nott, 1997; Nanayama et al., 2000; Nott, 2000, 2003).

6. Clast quarrying, entrainment and emplacement

6.1. Processes of dislodgement and emplacement related to extreme water levels

The study of the hydrodynamic conditions responsible for the clast transport was undertaken by analysing the 1989–1990 winter storms

Fig. 9. Shape and size of clast deposits. a) Upper part of the cliff fronting the south sector. Quarrying produces tabular clasts because of the joints pattern where horizontal joints are much larger than the vertical ones. Fresh sockets (X) in the centre of the view. b) Fresh socket and transported block on the scoured platform backing the cliff edge in front of cluster # 35. c) Rounded blocks at the base of the cliff fronting the central-south2 sector. White areas correspond to the bedrock and the blocks stripped of black lichen (*Verrucaria maura*) by polishing due to wave action. d) Largest clast located on the centre of the island (ridge #28) measuring 5.3 × 3.9 × 0.5 m and weighing approximately 32 t. (For interpretation of the references to colour in this figure legend, the reader is referred to the web version of this article.)

since important morphosedimentary and biological changes occurred during these events (Fichaut and Hallégouët, 1989). The emphasis was set on the extreme water level processes associated with wave runup since it has been described as a main parameter explaining the movement and the emplacement of large clasts and/or boulders (Dawson, 1994; Nott, 1997; Noormets et al., 2004). As explained earlier, the extreme water level was obtained by combining the measured tide level and the runup (Fig. 10). The results show that the

Table 2
Size and weight characteristics of cliff-top accumulations on Banneg.

	Index number of accumulation (see Fig. 7a)	Number of measured clasts	*a*-Axis	*b*-Axis	*c*-Axis	Volume (m^3)	Weight (t)
	#3	37	1.06	0.65	0.35	0.33	1.03
	#5 and #7	30	0.75	0.44	0.23	0.10	0.30
	#23C	72	0.76	0.49	0.24	0.12	0.38
	#24	100	1.27	0.84	0.31	0.52	1.60
	#28	145	1.43	0.95	0.39	0.69	2.15
	#29	17	1.71	1.21	0.51	1.09	3.38
	#30	103	0.99	0.58	0.28	0.22	0.69
	#31	87	1.25	0.75	0.34	0.49	1.52
	#32	60	1.18	0.78	0.34	0.38	1.18
	#33	40	1.09	0.69	0.30	0.37	1.14
	#34	50	1.03	0.64	0.27	0.20	0.61
	#35	82	1.08	0.65	0.30	0.27	0.84
	#36	11	1.44	0.87	0.46	0.65	2.01
	#37	63	1.07	0.67	0.29	0.27	0.83
	#44	11	2.05	1.21	0.45	1.30	4.02
Average			1.16	0.74	0.32	0.42	1.31
Standard deviation			0.57	0.40	0.15	0.81	2.50
		Dimensions A × B × C (m)					
Largest clast	#28	5.30 × 3.90 × 0.50				10.34	32.04
Smallest clast	#23C	0.40 × 0.20 × 0.05				0.004	0.01
Median clast	#35	0.80 × 0.60 × 0.40				0.19	0.6

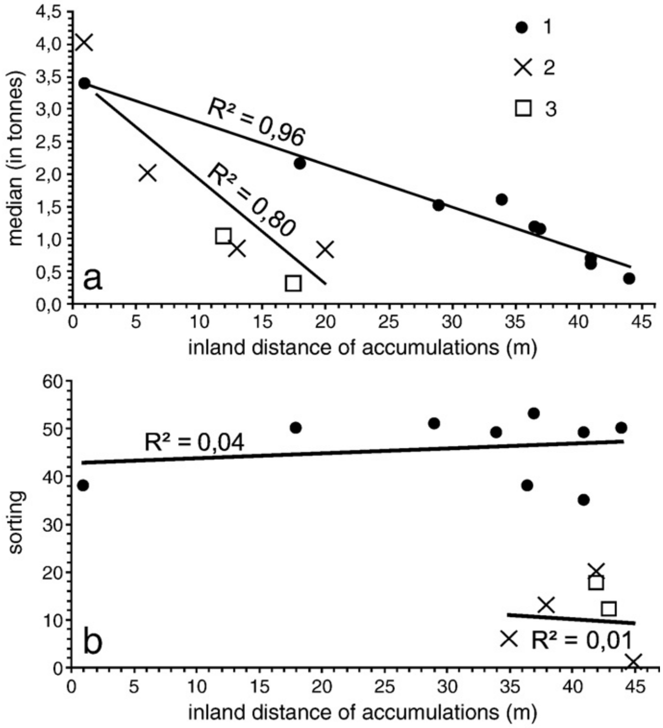

Fig. 10. a) Correlation between the size of the clasts (in tonnes) and the inland distance of the accumulations. b) Correlation between the sorting and the inland distance of the accumulations. 1. Accumulations in the central part of the island. 2. Accumulations in southern part of the island. 3. Accumulations in the northern part of the island.

16th of December, extreme water levels inducing submersion may have reached approximately 19 m high on the centre and the south of the island, that is to say 5 to 10 m higher than the top of sea-cliff (Fig. 10b). Considering the entire period, it appears that the submersion processes have been more frequent in the centre, the central–south1 and the south sectors then in the central-south2 sector where the height of the cliffs reaches 14 m. This could explain the smaller volume of clasts accumulated in the latter (Fig. 7c). On the contrary, only three events inducing cliff submersion were recorded on the north and the north–centre of the island (Fig. 10a). For the northern zone of the island, this pattern of storm flooding confirms minor impact reported by Fichaut and Hallégouët (1989), suggesting that the submersion processes were limited to a few meters inland (Fig. 11). On the other hand, in the north–centre zone, these results do not fit with the field observations showing that in this area, totally submerged by torrential flows, the turf was entirely removed and the scattered blocks were deposited in large amounts (Fig. 3b). It is difficult presently to explain these contradictory results in the north–centre sector. A further investigation on the link between foreshore morphology, orientation of the coast with respect to the main fetch, and hydrodynamic processes has to be carried out.

Finally, Fig. 10 shows that the highest extreme water levels calculated on the central part of the island (18.91 m), are higher than the maximum altitude of the clast deposits in this area (14.5 m on the central–south2 zone). This result fits with the observations reported by several authors, suggesting that the highest limit of the sediment accumulations always occurs below the runup upper limit (Dawson, 1994; Dawson and Shi, 2000; Nanayama et al., 2000).

6.2. Inventory of morphogenic events in the historical records

A 30-year inventory (1979–2007) of extreme events which could have generated powerful enough waves to detach and transport clast was compiled. The method used in this analysis was the same as the one used for the 1989–1990 winter storm events. The measured tide was combined to the runup in order to quantify the extreme water level of flood events. For calculation of this last parameter, wave data was obtained by numerical calculation.

Fig. 12 illustrates the main results of this analysis. The cyclicity of the curve is mainly due to seasonal variations of the waves characteristics. Peaks correspond to the strong swells of winter storms (December to February) whereas troughs correspond to a decrease in the heights and the periods of summer waves.

This time series also shows two periods regarding the extreme water levels. Thus the decade 1979–1989 (90) is characterized by a high frequency of morphogenic events whereas the following years (1990–2007), apart from 1993 and 1997, show a decrease of strong storms. Concerning surge levels at Brest, 11 to 16 years long cycles have been identified between 1860 and 1995 (Bouligand and Pirazzoli, 1999). This periodicity has been explained by shifts in the frequency of winds inducing surges in the past decades (Pirazzoli, 2000). These shifts could be attributed to the inversion from a negative towards a positive phase in the North Atlantic Oscillation index (Pirazzoli et al., 2004). However some authors have argued that this index by itself cannot explain all of the changes (Betts et al., 2004). This shift in number of morphogenic storms has also been pointed out in a recent study focusing on shoreline changes in southern Finistère, just south of the Iroise sea (Hallégouët and Hénaff, 2006). In this area all the beaches had chronic erosion between 1974–1990, because of numerous powerful storms, then entered a phase of regeneration which has mainly been attributed to the lack of strong storms since 1990.

The curve also demonstrates that no events as morphogenically significant as those of the winter of 1989–1990 were recorded during the other 28 years examined. In the central and southern parts of Banneg, the submersion episodes are particularly numerous during the first decade, the one of winter 1979–1980 being almost as important as the latter, with extreme water levels reaching 16 m. From 1990 to 2007, mainly after 1997, there is a sharp decrease in the scale and the number of storms. In the centre and the north–centre of the island, with the exception of the 1979–1980 and the 1989–1990 winter storms, the upper part of the cliffs was not submerged (Fig. 12b). However, in this case the calculation used in this study may minimize dynamic processes in the north–centre of the island.

7. Discussion

The arguments developed in the present study demonstrate that the cliff-top deposits on Banneg Island are the CTSDs as defined by Hall et al. (2006). These CTSDs are deposited on top of the western cliffs of the island or several meters inland from the cliff edge. They lay between 7.5 and 14 masl; the lowest altitude and latitude that these accumulations have been inventoried in northern Atlantic (Williams and Hall, 2004; Hall et al., 2006, 2008). The cliffs are facing the dominant swells and are fronted by deep waters. Immediately fronting the base of the cliffs the water depth reaches 50 m at 2000 m offshore. These depths are relatively weak as compared to the ones measured seaward of cliffs with the CTSDs in Orkney and Shetland. There they reach respectively 30 m and 50 m at 500 m from the base of the cliffs (Hall et al. 2006). Nevertheless, in Banneg, the fact that this area lacks a wide shore platform and/or skerries precludes the attenuation of the incoming waves. Therefore, the waves are capable of overtopping cliffs 8–14 m high and generating sufficient force on the cliff-top and scoured, supratidal platform to detach clasts, transport them and generate accumulations. Boulders in the deposits are mainly tabular, with sharp edges, unlike the ones accumulated at the base of the cliffs which are rounded. These blocks are therefore quarried from the upper cliffs or from the scoured platforms behind them. This is confirmed by the tabularity of the clasts that fits with the pattern of joints in the bedrock, where

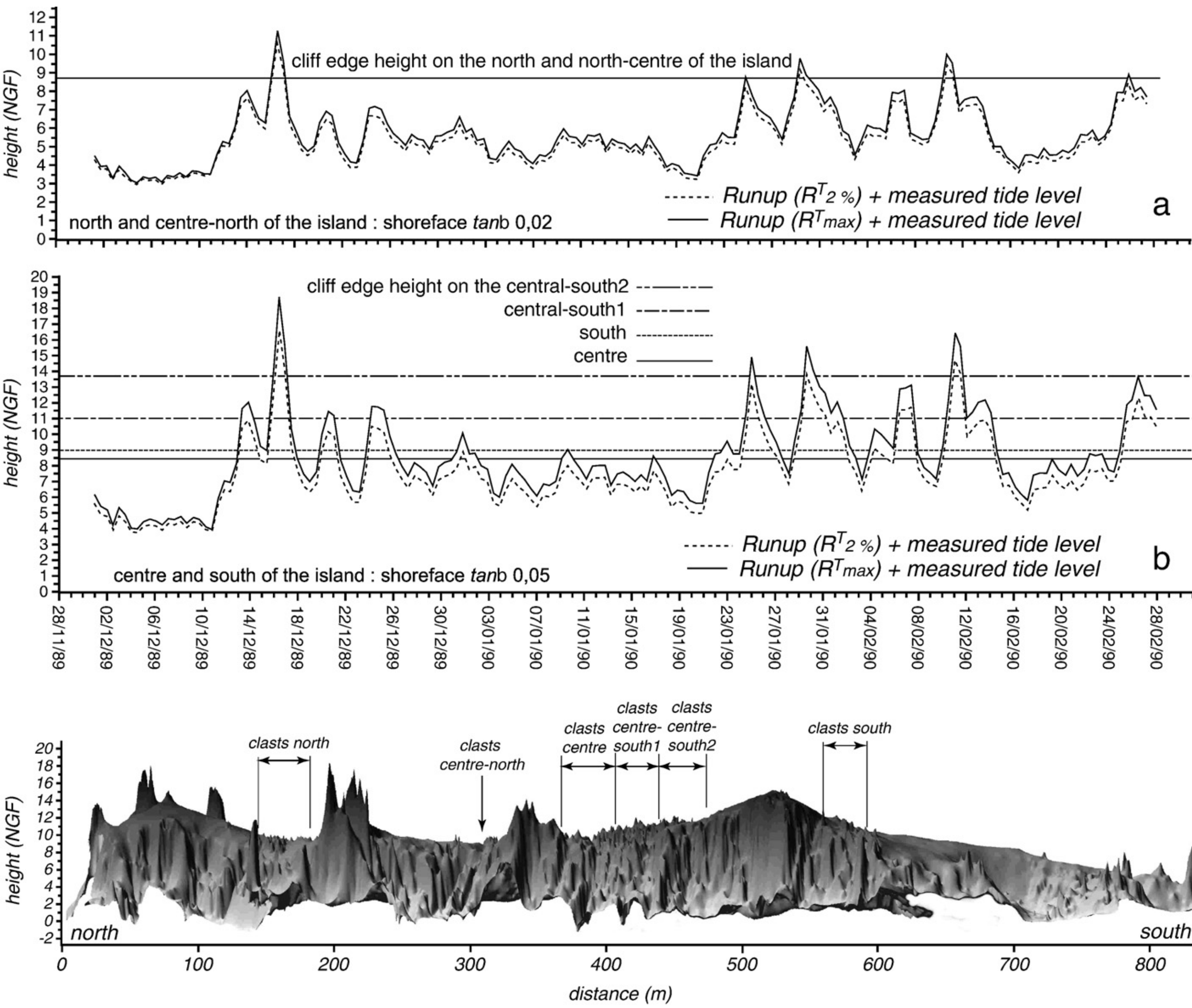

Fig. 11. Heights of extreme water levels (measured tide and runup) compared to sea-cliff heights during the 1989–1990 winter storms.

horizontal joints are much larger than the vertical ones. The altitude of sockets, from which boulders have been removed, ranges from 4 to 14 masl on the upper part of the cliffs or on the scoured platform.

Fig. 12. April 1990, the morphological and the biological impacts of the winter 1989–1990 storms in the northern part of the island. 1: limit of the vegetation degradation and soil erosion. 2: 9 m contour interval. 3: clasts deposited during the storm events. 4: scars of the clasts dislodged during the storms.

The accumulations vary in size and shape. The individual blocks, often embedded in vegetation have not been monitored in this study. Locally boulders form clusters (north–centre sector) which may form an arcuate set, parallel to the cliff edge (south sector). The most striking feature consists of ridges that occasionally form a sequence of three parallel ridges (centre sector). The latter is an argument used by several authors to explain that this type of accumulation is due to the repeated reworking by waves (Williams and Hall, 2004; Hall et al., 2006). As shown on Fig. 13, the North Atlantic storms, capable of producing waves high enough to overtop cliffs in the centre of Banneg occur almost annually. Another argument relating to the dip of clasts tends to prove that the accumulations on Banneg are storm surge deposits. The dip of clasts monitored on the seaward edge of the accumulations show that the dominant imbrication direction of the deposits varies from 270° to 330° corresponding to the dominant North Atlantic wind-driven storm wave direction.

This leads to one of the main debates relating to the origin of this type of high-energy deposit which compares the role of tsunami to storm waves (Jones and Hunter, 1992; Young et al., 1996; Nanayama et al., 2000; Nott, 2003; Noormets et al., 2004; Williams and Hall, 2004; Goff et al., 2006; Haslett and Bryant, 2007). In the present case, it is assumed that the North Atlantic storm waves play the key role. As exposed by Dawson et al. (2004), the trailing plate margin of the eastern North Atlantic is characterized by relatively few offshore earthquakes and weak volcanic activity, the two main sources of the tsunamis. The sole event of this type, the 1755 Lisbon tsunami, was generated by tectonics along the boundary between the African and the European plates. The impacts of this tsunami have been recorded all around the Atlantic but do not mention related cliff-top deposits (Andrade, 1992; Hindson et al., 1996; Dawson et al., 2004; Whelan and Kelletat, 2005; Haslett and Bryant, 2007). Another source of giant waves touching North the Atlantic and the Northern Sea coasts correspond to the underwater sediment slumps on the Norwegian continental slope (Dawson et al., 1988; Bondevik et al., 1997; Dawson, 1999; Bondevik et al., 2005). Moreover, other high-energy events occurred in the Medieval Warm Period and the Little Ice Age (Haslett and Bryant, 2007). However, as explained by Dawson et al. (2004), these uncommon and ancient events cannot by themselves explain the large amount of cliff-top deposits found along the exposed coasts of Northern Europe. The present study reinforces the idea, which is increasingly accepted, that oceanic storms may generate accumulations similar to those of the tsunamis (Einsele et al., 1996; Nott, 1997; Gentile et al., 2003; Nott, 2003; Noormets et al., 2004; Hall et al., 2006). An argument, relating to the runup values, could challenge the role of storms in the edification of boulder deposits on Banneg. The values of the runup on Banneg are close to the ones generated by the giant tsunami waves. On the northern coast of Oahu (Hawaii) Noormets et al. (2002) indicate that the runup generated by the tsunamis of the last two centuries ranged between 1.8 and 10.7 m. In the same area, Whelan and Keating (2004) calculated that the 9 to 11 m high waves associated with the Aleutian tsunami of 1946 produced a 9.3 m runup that entirely submerged the oriental coastal plain of the island. According to Bondevik et al. (2005), on the Shetland Islands, the height of the runup generated by the Holocene tsunamis ranged in between 7 and 25 m depending on the sites.

The maximum height of the waves recorded in our study area reached 22 m during the 1989–1990 winter storms, but generated a maximum runup ranging between 7–13.5 masl. The maximum height of the waves recorded reaches 24.3 m in the Shetland Islands (Hall et al., 2006) and 29.1 m in Scotland (Holliday et al., 2006). They generated a wave runup that reached 50 masl. As mentioned earlier, this difference is due to the depth of waters fronting the cliffs. Where depth reaches 30 m and 50 m at 500 m from the base of the cliffs respectively in Orkney and Shetland (Hall et al. 2006) they reach 50 m at 2000 m from the coast of Banneg. Therefore the slope offshore is steeper in the British isles than in Banneg, hence the runup is more important. Storms generate waves capable of quarrying joint bounded blocks reaching several tons. In the case of Banneg Island, the median and maximum size and weight is respectively $0.8\times0.6\times0.4$ m (0.6 t) and $5.3\times3.9\times0.5$ m (32 t). These sizes are much smaller than what has been recorded at other locations. The maximum weight reaches 120 t in Northern Scotland or in the Shetland Islands on the North Sea, 250 t in Northern Ireland (Williams and Hall, 2004), 860 t on the Aran Islands (Hall et al., 2006). Blocks up to 90 t were recorded on Oahu Island Hawaii (Noormets et al., 2002), the largest blocks being measured on the Tuamotu Islands, 1500 t (Bourrouilh-Le Jan and Talandier, 1985) or on the Bahamas, 2300 t (Hearty, 1997). However, as demonstrated by several authors, the size of the transported blocks does not depend exclusively on the strength of the waves but is also the function of the lithofacies and of the pattern of faults and cracks that may be a key factor for the quarrying of blocks by the waves. In the Tuamotu, Bourrouilh-Le Jan and Talandier (1985) have shown that because cracks were rare, the quarrying was spatially limited to the particular locations within the outcrop. Comparable observations were made by Jones and Hunter, 1992 on the Grand Cayman Island in the Caribbean, and on Oahu (Noormets et al., 2002), where quarried blocks came from densely jointed areas. On Banneg, the variability of the size and the volume of blocks are controlled by this parameter. Among the 908 blocks monitored, 25 only exceed 6 t (2 m^3). These large clasts correspond to the rock heads or the outcrops that have been flipped whereas all the others fit with the pattern of joints in the bedrock. The granulometric and the morphometric data of boulders are comparable to the results obtained on other sites. The dwindling of block sizes inland is commonly noticed on other sites (Moore and Moore, 1984; Bourrouilh-Le Jan and Talandier, 1985; Bryant et al., 1992; Nott, 1997; Nanayama et al., 2000; Nott, 2000, 2003; Scheffers and Kelletat, 2004;

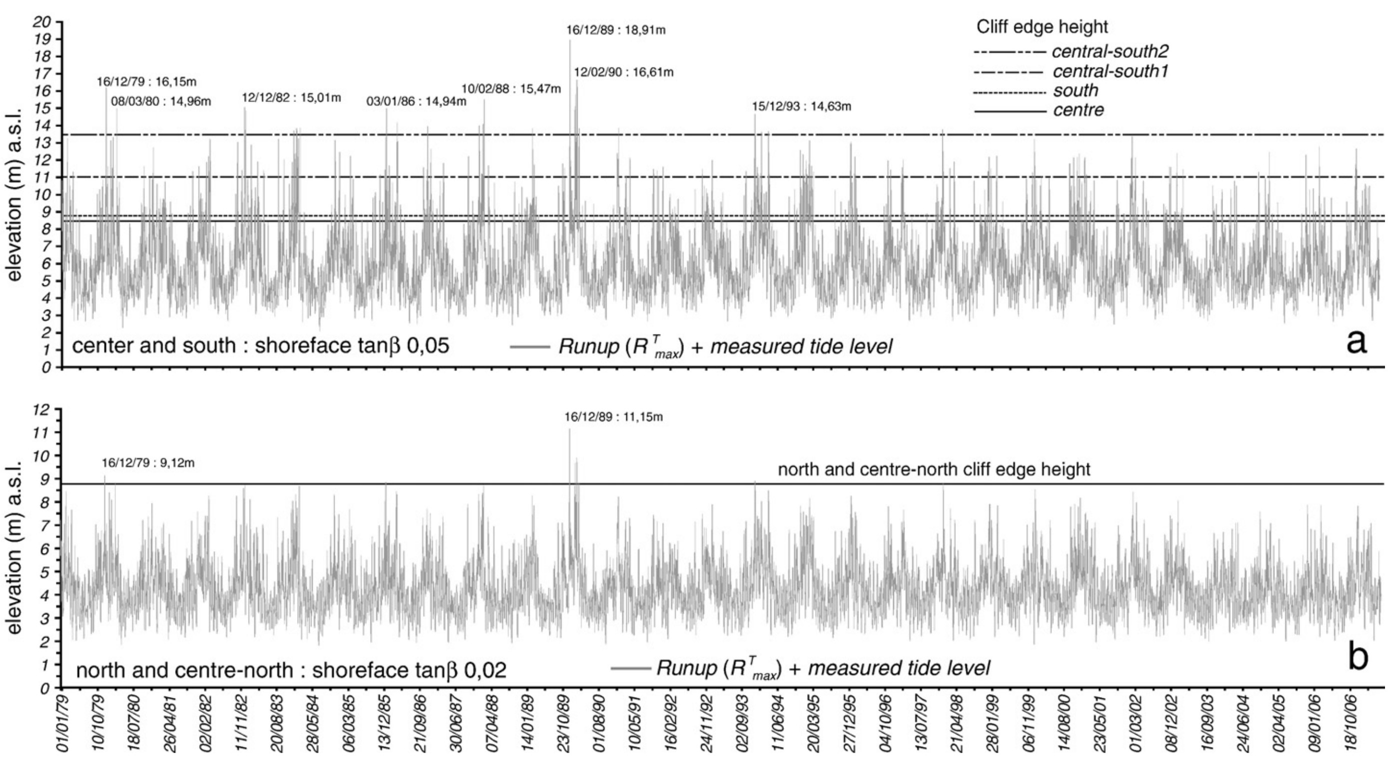

Fig. 13. Heights of extreme water levels (measured tide and runup) compared to sea-cliff heights from January 1st 1979 and June 7th 2007.

Goff et al., 2006). On the contrary, there is no sorting of clasts landward as usually occurs in case of a tsunami when the grain size decreases landward because of the loss of velocity and mass of the wave (Nanayama et al., 2000). This raises questions about the origin and the chronology of the dynamic processes. On Banneg, the deposits are the result of several storms characterized by different levels of energy. Differences in runup values depend on the variability of the wave heights from one storm to the other. They may explain the reworking of the accumulations located at different distances from the cliff edge. These processes have been precisely described by Hall et al. (2008) on Grind of the Navir cliffs in the Shetland where runup flowing over the top of the cliff may get airborne, spare some deposits on the cliff edge and rework others inland. Therefore, as explained by Hall et al. (2006), the accumulations which have been reworked by successive storms are characterized by the mixing of clasts.

Historical records of the extreme water level during the last thirty years do not allow us to establish a relevant chronology of the events responsible for their deposition. Based on our present data, we can only claim that the major storms of 1989–1990 winter storms have generated an important sedimentation and that other storms have reworked some blocks or ridges. However, the features such as the imbricate clast trains or the triple ridges laying in the centre of the island are the likely result of the morphogenic events that occurred prior to the period of survey.

8. Conclusion

The cliff-top accumulations inventoried on Banneg Island provide additional evidence of the strength of the major storms in the Northern Atlantic to cause block detachment and transport. The accumulations on Banneg Island can therefore be considered as CSTDs as defined by Hall et al. (2006). Features that appear to distinguish CTSDs from tsunami deposits include the development of imbricate clasts forming ridges. As noted by Williams and Hall (2004), this organisation into ridges, possibly triple ridges as on Banneg, may require repeated reworking by waves rather than the rare impact of a single train of tsunami waves. Imbricate fabric has been also interpreted as repeated accumulation processes due to storm waves. Morphological and sedimentary characteristics of these deposits show that their set up is controlled by a combination of key points:

- the cliffs facing west and fronted by deep water receiving extreme waves slightly modified from the deep ocean
- a bedrock with well defined joint and bedding planes enhancing the detachment of fracture-bounded tabular blocks
- the clasts correspond to tabular blocks which are mostly quarried from the upper part of the cliff and the scoured platform
- the wave-derived bores of water overtopping the top of the cliffs corresponding to deep-sea waves exceeding 20 m.

The detailed configuration of the coast, particularly the size, the height, the orientation and the form of the cliff edge and top, exerts a major control on the distribution, the altitude, the clast orientation and the clast size of the cliff-top deposits. The CTSDs of Banneg Island are typically located directly inland of coves separated by headlands, which concentrate the wave energy, creating favourable conditions for block detachment and entrainment. The differences in size of the imbricated clasts, the largest ones in the centre and the central–south1 areas opposed to the smallest ones southward and northward, may be explained by the fact that from the north to the south of the island, individual cells can be distinguished by their own morphodynamic functioning, mainly related to the morphology of the offshore zone front of the cliff.

Over the last 30 years, the storms of winter of 1989–1990 have generated the most significant morphogenic changes in terms of erosion and reworking. The decade between 1979 and 1990 was characterized by high intensity storms, possibly responsible for the minor reworking of the CTSDs, were more numerous than during the following period (1991–2007). With the prospect of climatic change due to the global warming, sea level rise as well as the potential increase in storm frequency could accentuate hydrodynamic and morphosedimentary processes. As such, these morphologic features appear to be a good indicator of climatic and/or meteo-oceanic variations on the short and long term.

Acknowledgements

The authors wish to thank the DIREN Bretagne that founded this work. Access to the island was made possible with the help of J.-Y. Le Gall and D. Bourlès rangers of the Réserve Naturelle D'Iroise. The wave data came from Atlas Numérique de Mer Océanique et côtier (ANEMOC) and from the records of the lighthouse-buoy BEAIII, and were provided respectively by F. Lafon, M. Benoît, J.C. Fournier from LNHE-EDF and G. Goasguen from CETMEF-Brest. Tide data was at our disposal thanks to B. Simon and R. Jehan from SHOM-Brest.

References

Andrade, C., 1992. Tsunami generated forms in the Algarve barrier islands. Sci. Tsunami Hazards 10 (1), 21–34.
Battjes, J.A., 1974. Surf similarity. Proceeding of the 14th Coastal Engineering Conference. Amer. Soc. Civil Engrs, pp. 466–479.
Betts, N.L., Orford, J.D., White, D., Graham, C.J., 2004. Storminess and surges in the south-western approaches of the eastern North Atlantic: the synoptic climatology of recent extreme coastal storms. Mar. Geol. 210 (1–4), 227–246.
Bondevik, S., Svendsen, J.-I., Mangerud, J., 1997. Tsunami sedimentary facies deposited by the Storegga tsunami in shallow marine basins and coastal lakes, Western Norway. Sedimentology 44 (6), 1115–1131.
Bondevik, S., Mangerud, J., Dawson, S., Dawson, A., Lohne, Ø., 2005. Evidence for three North Sea tsunamis at the Shetland Islands between 8000 and 1500 years ago. Quat. Sci. Rev. 24 (14–15), 1757–1775.
Bouligand, R., Pirazzoli, P.A., 1999. Les surcotes et les décotes à Brest, étude statistique et évolution. Oceanol. Acta 22 (2), 153–166.
Bourrouilh-Le Jan, F.G., Talandier, J., 1985. Sedimentation et fracturation de haute énergie en milieu récifal : tsunamis, ouragans et cyclones et leurs effets sur la sédimentation et la géomorphologie d'un atoll : Motu et Hoa, à Rangiroa, Tuamotu, Pacifique SE. Mar. Geol. 67 (3–4), 263–333.
Bryant, E.A., Young, R.W., Price, D.M., 1992. Evidence of tsunami sedimentation on the southeastern coast of Australia. J. Geol. 100, 753–765.
Dawson, A.G., 1994. Geomorphological effects of tsunami run-up and backwash. Geomorphology 10 (1–4), 83–94.
Dawson, A.G., 1999. Linking tsunami deposits, submarine slides and offshore earthquakes. Quat. Int. 60 (1), 119–126.
Dawson, A.G., Shi, S., 2000. Tsunami deposits. Pure Appl. Geophys. 157, 875–897.
Dawson, A.G., Long, D., Smith, D.E., 1988. The Storegga slides: evidence from eastern Scotland for possible tsunami. Mar. Geol. 82 (3–4), 271–276.
Dawson, A.G., Lockett, P., Shi, S., 2004. Tsunami hazards in Europe. Environ. Int. 30 (4), 557–585.
Einsele, G., Chough, S.K., Shiki, T., 1996. Depositional events and their records—an introduction. Sediment. Geol. 104 (1–4), 1–9.
Fichaut, B., Hallégouët, B., 1989. Banneg : une île dans la tempête. Penn ar Bed 135, 36–43.
Gentile, G., Mastronuzzi, G., Sansò, P., 2003. Using boulders accumulations as tsunami indicators: an hydrodynamic approach, GI²S Coast. Res. Publ. 4, 99–101.
Goff, J., Dudley, W.C., deMaintenon, M.J., Cain, G., Coney, J.P., 2006. The largest local tsunami in 20th century Hawaii. Mar. Geol. 226 (1–2), 65–79.
Guilcher, A., 1959. L'archipel de Molène (Finistère). Etude morphologique. Rev. Géogr. Phys. Géol. Dyn. II (2), 81–96.
Hall, A.M., Hansom, J.D., Williams, D.M., Jarvis, J., 2006. Distribution, geomorphology and lithofacies of cliff-top storm deposits: Examples from the high-energy coasts of Scotland and Ireland. Mar. Geol. 232 (3–4), 131–155.
Hall, A.M., Hansom, J.D., Jarvis, J., 2008. Patterns and rates of erosion produced by high energy wave processes on hard rock headlands: the Grind of the Navir, Shetland, Scotland. Mar. Geol. 248 (1–2), 28–46.
Hallégouët, B., 1982a. Géomorphologie de l'archipel de Molène. Penn ar Bed 110, 83–97.
Hallégouët, B., 1982b. L'archipel de Molène. Penn ar Bed 110, 79–82.
Hallégouët, B., 1984. Contribution à l'étude morphologique de l'archipel de Molène (Finistère. Actes du 107ème Congrès National des Sociétés Savantes, Brest 1982, Secteur de Géographie, Etudes géographiques sur la Bretagne et questions diverses. CTHS, Paris, pp. 61–77.
Hallégouët, B., Hénaff, A., 2006. Evolution récente et gestion des espaces littoraux de l'ouest Cornouaille, Les Actes des rencontres de l'ouest Cornouaille. « Quelles pistes de développement pour le territoire ? », Mai – juin 2005. Association Ouest Cornouaille Promotion (AOCP), Pont-L'Abbé, pp. 20–34.
Hansom, J.D., Hall, A.M., 2009. Magnitude and frequency of extra-tropical North Atlantic cyclones: a chronology from cliff-top storm deposits. Quart. Int. 195 (1–2), 42–52.
Hansom, J.D., Barltrop, N.D.P., Hall, A.M., 2008. Modelling the processes of cliff-top erosion and deposition under extreme storm waves. Mar. Geol. 253 (1–2), 36–50.

Haslett, S.K., Bryant, E.A., 2007. Reconnaissance of historic (post-AD 1000) high-energy deposits along the Atlantic coasts of southwest Britain, Ireland and Brittany, France. Mar. Geol. 242 (1–3), 207–220.
Hearty, P.J., 1997. Boulder deposits from large waves during the last interglaciation on North Eleuthera Island, Bahamas. Quat. Res. 48 (3), 326–338.
Hindson, R.A., Andrade, C., Dawson, A.G., 1996. Sedimentary processes associated with the tsunami generated by the 1755 Lisbon earthquake on the Algarve coast, Portugal. Phys. Chem. Earth. 21 (12), 57–63.
Holliday, N.P., Yelland, M.J., Pascal, R., Swail, V.R., Taylor, P.K., Griffiths, C.R., Kent, E., 2006. Were extreme waves in the Rockall Trough the largest ever recorded? Geophys. Res. Lett. 33, L05613.
Jones, B., Hunter, I.G., 1992. Very large boulders on the coast of Grand Cayman: the effects of giant waves on rocky coastlines. J. Coast. Res. 8 (4), 763–774.
Mase, H., 1989. Random wave runup height on gentle slopes. Journal of Waterway, Port, Coastal, and Ocean Engineering 115 (5), 649–661.
Moore, J.G., Moore, G.W., 1984. Deposit from a giant wave on the island of Lenai, Hawaii. Science 226, 1498–1499.
Nanayama, F., Shigeno, K., Satake, K., Shimokawa, S., Miyasaka, S., Ishii, M., 2000. Sedimentary differences between the 1993 Hokkaido-nansei-oki tsunami and the 1959 Miyakojima typhoon at Taisei, southwestern Hokkaido, northern Japan. Sediment. Geol. 135 (1–4), 255–264.
Noormets, R., Felton, E.A., Crook, K.A.W., 2002. Sedimentology of rocky shorelines: 2. Shoreline megaclasts on the north of Oahu, Hawaii — origins and history. Sediment. Geol. 150 (1–2), 31–45.
Noormets, R., Crook, K.A.W., Felton, E.A., 2004. Sedimentology of rocky shorelines: 3. Hydrodynamics of megaclast emplacement and transport on a shore platform, Oahu, Hawaii. Sediment. Geol. 172 (1–2), 41–65.
Nott, J., 1997. Extremely high-energy wave deposit inside the Great Barrier Reef, Australia: determining the cause — tsunami or tropical cyclone. Mar. Geol. 141 (1–4), 193–207.
Nott, J., 2000. Records of prehistoric tsunamis from boulder deposits — evidence from Australia. Sci. Tsunami Hazards 18 (1), 3–14.
Nott, J., 2003. Tsunami or storm waves? — determining the origin of a spectacular field of wave emplaced boulders using numerical storm surge and wave models and hydrodynamic transport equations. J. Coast. Res. 19 (2), 348–356.
Pirazzoli, P.A., 2000. Surges, atmospheric pressure and wind change and flooding probability on the Atlantic coast of France. Oceanol. Acta 23 (6), 643–661.
Pirazzoli, P.A., Régnauld, H., Lemasson, L., 2004. Changes in storminess and surges in western France during the last century. Mar. Geol. 210 (1–4), 307–323.
Scheffers, A., Kelletat, D., 2004. Bimodal tsunami deposits — a neglected feature in paleo-tsunami research. In: Schernewski, G., Dolch, T. (Eds.), Geographie der Meere und Küsten: Coastline Reports, vol. 1, pp. 67–75.
Whelan, F., Keating, B., 2004. Tsunami deposits on the island of Oahu, Hawaï'ï. In: Schernewski, G., Dolch, T. (Eds.), Geographie der Meere und Küsten: Coastline Reports, vol. 1, pp. 77–82.
Whelan, F., Kelletat, D., 2005. Boulder deposits on the southern Spanish Atlantic coast: possible evidence for the 1755 AD Lisbon tsunami? Sci. Tsunami Hazards 23 (3), 25–38.
Williams, D.M., Hall, A.M., 2004. Cliff-top megaclasts deposits of Ireland, a record of extreme waves in the North Atlantic-storms or tsunamis? Mar. Geol. 206 (1–4), 101–117.
Young, R.W., Bryant, E.A., Price, D.M., 1996. Catastrophic wave (tsunami?) transport of boulders in southern New South Wales, Australia. Z. Geomorphol. 40, 191–207.